Available online at www.sciencedirect.com
ScienceDirect
Cement and Concrete Research 37 (2007) 139–150
Cement and Concrete Research

Enhanced thermodynamic analysis coupled with temperature-dependent microstructures of cement hydrates

Kenichiro Nakarai [a,*], Tetsuya Ishida [b], Toshiharu Kishi [c], Koichi Maekawa [b]

[a] Department of Civil Engineering, Gunma University, 1-5-1 Tenjin-cho, Kiryu-shi, Gunma, Japan
[b] Department of Civil Engineering, The University of Tokyo, 7-3-1 Hongo, Bunkyo-ku, Tokyo, Japan
[c] Institute of Industrial Science, The University of Tokyo, 4-6-1 Komaba, Meguro-ku, Tokyo, Japan

Received 1 October 2005; accepted 4 October 2006

Abstract

This paper describes a computational method for simulating concrete performance. The method is enhanced to take into account the influence of the curing temperature history on the early-age development process. In order to investigate the effect of temperature on hydration, micro-pore structure development, and moisture profile in concrete, the authors carried out systematic sensitivity analyses. These analyses were used to create a numerical model that takes into account the temperature-dependent intrinsic porosity of hydrates and the available space for hydrate precipitation. For example, at high curing temperatures, the intrinsic porosity decreases and the available space for hydration increases. Experiments verified that the proposed method accurately predicts hydration processes, microstructure formation, and relative humidity for different mix proportions under various temperatures. Compared with the conventional model, the new model offers greater overall computational accuracy for low W/C and high temperature curing.

Keywords: Hydration; Cement hydrate; Temperature; Free water; Pore structure; Low W/C

1. Introduction

In order to rationally design, construct, maintain, and retrofit RC structures, it is necessary to first predict the long-term material performance of the concrete. The thermodynamic analytical system, called DuCOM, simulates concrete behaviors during the hardening stage [1] and deterioration during the long-term service period [2]. The system consists of three basic models: a multi-component cement hydration model, a micro-pore structure development model, and a moisture transport/equilibrium model. Their strong interrelationships are taken into account by real-time sharing of material characteristic variables across each model. The input information required by the model are mix proportion, mineral composition of cement, geometrical shape of structure, initial temperate and environmental boundary conditions. The key parameters such as porosity distribution, permeability of concrete are simulated in the computation based on physicochemical characteristics of concrete. This means that the analytical scheme can be generalized method for assessing concrete performance under arbitrary mix proportions and environmental conditions.

One of the most important issues in the assessment of concrete performance is to evaluate the effect of temperature on the material properties of concrete. In the cases of mass concrete or low W/C concrete, the inner temperature of the RC structure can reach 70–80 °C, which increases the risk of thermal cracking. In order to evaluate the risk of cracking and the long-term properties of the concrete, which experiences high temperatures early in its service life, the analytical system must be enhanced so that it can be applied to a wide range of temperatures.

In the hydration model of the thermodynamic system (DuCOM) [1], the referential hydration heat rate and activation energy of each mineral compound are defined in a manner that considers the temperature dependency. In the moisture transport/equilibrium model, the temperature and time dependencies of the inkbottle effect and the interlayer water were modeled [3]. In the microstructure model, however, temperature dependency was not taken into account despite experiments showing that the curing temperature strongly influences the properties of the

* Corresponding author. Tel.: +81 277 30 1611; fax: +81 277 30 1601.
E-mail address: nakarai@ce.gunma-u.ac.jp (K. Nakarai).

0008-8846/$ - see front matter © 2006 Elsevier Ltd. All rights reserved.
doi:10.1016/j.cemconres.2006.10.006

hydration products and the formed microstructure [4–6]. The influence of temperature on the micro-pore structure needs to be investigated and considered in the model.

In addition, Kishi et al. [7] revealed that the hydration process for low W/C concrete under adiabatic temperature conditions differs from that for normal W/C concrete containing adequate water for hydration. The peculiar behavior of low W/C concrete was tentatively explained by the increase in free water for hydration due to the decrease in absorbed water associated with self-desiccation. The additional investigation from the viewpoint of microstructure, however, is necessary since the high temperature under adiabatic temperature condition may affect microstructure.

In this study, the influence of temperature on the development of the micro-pore structure, the moisture profile, and the hydration process and their mutual interactions are investigated. Subsequently, the thermodynamic analytical system was enhanced to provide higher accuracy and wider applicability.

2. Temperature dependency in the analytical system and sensitivity analysis

2.1. Redefinitions of pores in the DuCOM analytical system

In the conventional DuCOM model [1], the pores in the cement paste were classified into three types: interlayer, gel pore, and capillary pore. They were determined according to whether or not the pore space was available for precipitating cement hydrate. Interlayer and gel pores are formed with cement hydrates during the hydration process and are unavailable for hydrate precipitation. Capillary pores are free spaces for the precipitation of hydrates. These definitions are based on the Powers–Brownyard model [8], which defines a gel pore as a pore in hydrate products and a capillary pore as the remnant of an initially water-filled space. In this paper, the gel pore includes the gel pore and interlayer pore from the conventional DuCOM model, as shown in Table 1. And, as proposed by Taylor, “hydration product” replaces “cement gel” in the Powers–Brownyard gel-pore model since the hydration product includes crystals of calcium hydroxide (CH) [9].

Since the gel pore in the Powers–Brownyard model consists of different kinds of pores (interlayer, micro, and fine meso pores) according to Taylor [9], which differs somewhat from the general definition that is associated with pore size [10,11], the definitions of pores in this study need to be clarified before discussing the enhanced model. In this paper, the gel pore in the conventional DuCOM model is redefined as two kinds of pores: an intra-gel pore and an inter-hydrate pore (Table 1). This redefinition is necessary for discussing the macroscopic characteristics such as hydration and the porosity distribution of concrete materials for arbitrary thermal actions.

The intra-gel pores are assumed to be located inside the cement gel, while the inter-hydrate pores are assumed to be located in the spaces between the hydrate products, which include C–S–H gel and CH. In the definition based on pore size (Table 1), the intra-gel pores in this paper correspond to the smaller gel pores in the conventional DuCOM that have a radius smaller than around 2 nm. The inter-hydrate pores in this study correspond to the larger gel pores in the conventional DuCOM that have a radius larger than around 2 nm. The inter-hydrate and capillary pores in this paper correspond to the capillary pores described by Uchikawa [11].

The intra-gel and inter-hydrate pores are basically considered to be dead space for precipitating new hydrate products, similar to the gel pore in the conventional DuCOM. In order to evaluate the material performance of concrete under arbitrary temperature histories, this paper focuses on the additional functions of the inter-particle pores as free space for the precipitation of hydrate products under high temperatures.

2.2. Outline of the DuCOM analytical system and issues

This section briefly introduces the DuCOM analytical system and discusses issues associated with temperature dependencies using the redefinitions of pores proposed in the previous section.

2.2.1. Multi-component cement hydration model and free water for hydration

In the multi-component cement hydration model [1], the referential hydration heat rate and activation energy in the equation of reaction kinetics are defined in a manner that considers the temperature dependency. Mutual interactions among the reacting constituents during hydration are quantitatively formulated. The effect of free water on the hydration rate is modeled using the hard shell concept of a hydrated cluster. The degree of heat generation rate decline in terms of both the amount of free water and the thickness of internal hydrates layer is formulated. The amount of free water can be calculated from the microstructure and the moisture distribution. In the conventional

Table 1
Classification of pores

Powers and Brownyard [8]	Taylor [9]	Daimon [10]	Uchikawa [11]	Conventional DuCOM [1]	Modified DuCOM
Gel	Interlayer	Intra-crystallite (<0.6 nm)		Interlayer	Interlayer
	Micro (<2 nm)	Inter-crystallite (0.6–1.6 nm)	Gel (0.5–1.5 nm)	Gel	Intra-gel
	Fine meso (>2 nm)	Inter-gel particle (1.6–100 nm)	Capillary (1.5 nm–15 μm)		Inter-hydrate
Capillary				Capillary	Capillary

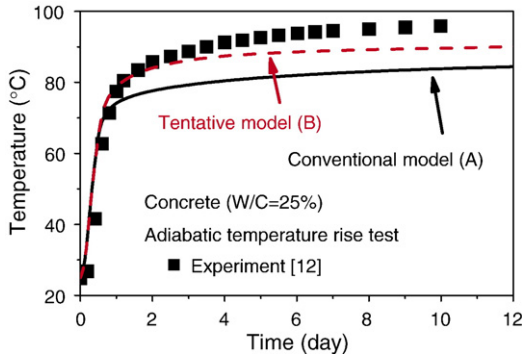

Fig. 1. Hydration process under adiabatic temperature condition.

model [1], only the condensed water in the capillary pores was considered as free water for hydration (Model A).

Recently, Kishi et al. tentatively proposed an enhanced model that added a part of the moisture in the inter-hydrate pores to the free water and considered the change of adsorbed water associated with relative humidity (Model B) [7]. The purpose of this proposal was to explain the continuous hydration process of low W/C concrete under adiabatic temperature conditions. The large temperature rise was predicted by considering the increase in the amount of free water for hydration. In calculating the amount of free water in Model B, the following water is assumed to be constrained water that cannot be used for hydration.

- The water in inter-hydrate pores that have a radius of *hydRmin* or smaller
- A part of the condensed water present within 1 nm of the walls of saturated inter-hydrate and capillary pores
- The absorbed water in unsaturated pores
- The interlayer water and the water in the intra-gel pores.

Here, *hydRmin* is the minimum radius of the available space in an inter-hydrate pore for hydrate precipitation. It was tentatively assumed to be 1.0 nm in Model B.

The hydration models can be verified by measuring the heat generated in the adiabatic temperature rise test or by performing thermo gravimetric analysis (TGA) of the chemically bound water. For normal W/C (above approx. 40%), both models produce the same degree of hydration since enough free water is present for hydration. The applicability of the hydration model for the normal W/C concrete has been already verified through a comparison with the results of several experiments (W/C=38.0–78.5%) [1]. On the other hand, for low W/C, the two models produce different results due to the lack of free water. Fig. 1 shows the test results of an experiment and an analysis of adiabatic temperature rise in the case of concrete T25 (W/C=25%) [12]. The analysis shows that Model B generated more heat than Model A. The continuous hydration result from the analysis of Model B is calculated from the increase in the amount of free water. Fig. 2 shows the results of the experiment and analysis of bound water in cement paste Y30 (W/C=30%) [1]. The analysis shows that Model B had higher hydration than Model A. However, the value is too large when compared to the result of the experiment inversely with the adiabatic temperature rise test. The differences in the results for heat generation and bound water can be explained by the differences in the conditions of the experiment. While the temperature of the specimen in the adiabatic temperature test exceeded 90 °C, the specimen in the bound water test was cured at a temperature of 20 °C. Since the curing temperatures in the two tests were very different, the effects of different curing temperature must be investigated. This temperature dependency is a key issue in this study. The mix proportions of T25 and Y30 are shown in Table 2.

Table 2
Mix proportion of concrete and paste and mineral component of cement

No.	Ref.	W/C (%)	Unit mass (kg/m^3)				Mineral component			
			W	C	S	G	C_3S	C_2S	C_3A	C_4AF
T25	[12]	25	150	600	876	730	40.4	37.7	3.9	11.8
Y30	[1]	30	485	1620	0	0	49.7	23.9	8.8	3.4
P25	–	25	440	1762	0	0	54.4	19.9	9.4	8.8
25N	[16]	25	441	1765	0	0	60.6	14.2	8.2	8.9

2.2.2. Moisture transport/equilibrium model

In the moisture model [1], the pore pressure, relative humidity, and moisture distribution are mathematically simulated using a moisture transport model that considers both the vapor and liquid phases of mass-transport as defined by thermodynamics. The moisture dispersed in the capillary, intra-gel, inter-

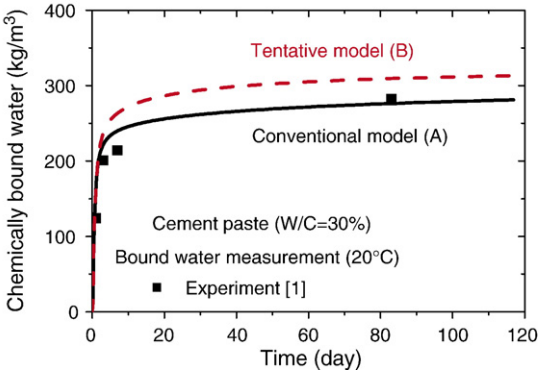

Fig. 2. Hydration process under normal temperature condition (20 °C).

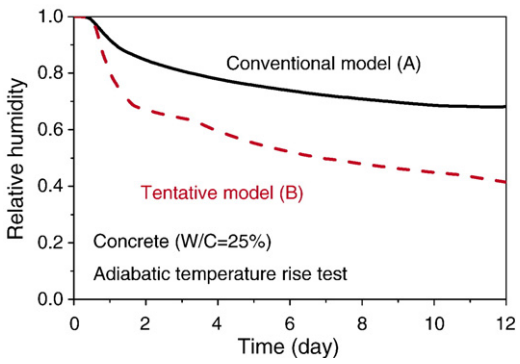

Fig. 3. Relative humidity under adiabatic temperature condition.

hydrate and interlayer pores in the cement hydrate are classified as condensed water, absorbed water, or interlayer water. They are modeled according to their properties. The hysteresis behaviors of isotherms under cyclic drying–wetting conditions take into account the inkbottle effect in the capillary, intra-gel and inter-hydrate pores and the process of dispersing the interlayer water.

Figs. 3 and 4 show the results of an analysis of the relative humidity in concrete T25 and cement paste Y30, respectively. The relative humidity calculated by Model B is lower than that calculated by Model A. It is also lower than the published results of other experiments. For example, Persson reported that the relative humidity of low W/C concrete (W/C=25%) was around 75% after 450 days under sealed conditions [13]. Park and Noguchi showed that the relative humidity increased as the curing temperature rose; the humidity at 2 days was around 90% at 60 °C [14]. Therefore, it is necessary to investigate the validity of the calculated relative humidity at the end of the hydration process by considering the temperature dependency of the microstructure and moisture profile [7].

Recent research [3] has produced a temperature dependent hysteresis model based on the results of experiments. In the enhanced model, the water trapped by the inkbottle effect is redefined as water that can gradually disperse according to the temperature of the pore system. The rate of the change of the parameter, which numerically expresses the time-dependent dispersion of inkbottle water, is dependent on temperature and is influenced by the ambient humidity. The sensitivity to temperature and humidity was back-analyzed through finite element analysis consistent with the test conditions. The rate of loss of the trapped water increases at higher temperatures and lower humidity. The proposed model has been verified by comparing the results with those of experiments on moisture loss in concrete under high temperatures. In the adiabatic temperature test (T25) discussed in this paper, high curing temperatures can affect the moisture profile. Therefore, it is necessary to use the proposed temperature-dependent model to investigate the effect of temperature.

Also proposed is a temperature-dependent model for the interlayer water. This model is based upon the results of experiments [3]. In order to expand the scope of application to cover a wider range of temperature conditions, a function for expressing an envelope curve on the moisture isotherm of interlayer water has been introduced.

Table 3
Evaluation of calculation results in case of low W/C

Temperature condition	Index	Model A	Model B
Adiabatic (High temperature)	Heat generation	Underestimate	Good
	Relative humidity	Underestimate	Underestimate
20 °C (Normal temperature)	Bound water	Good	Overestimate
	Relative humidity	Good	Underestimate

2.2.3. Micro-pore structure formation model

The microstructure model [1] assumes monosized particle dispersion and uses a particle expansion model. It is based on the degree of hydration and the amount of chemically bound water calculated by the hydration model. The effect of particle size is taken into account as the effect of average distance between particles. Assuming linear variations in porosity in the expanding cluster, the pore size distributions are computed over time.

In this calculation, the microstructure model uses parameters that represent the properties of hydrates, such as the density of the bound water and the specific surface area of the gel particles. The temperature dependencies of the properties are not considered in the conventional model [1] although other researchers have reported on them [4–6]. The effect of the temperature dependencies on the formed microstructure will be discussed in this paper. The intrinsic porosity will be one of the most important parameters in the micro-pore structure model.

The intrinsic porosity of the hydrates includes the intra-gel, inter-hydrate, and the interlayer porosity. The porosity is defined as the volume ratio of the intra-gel, inter-hydrate, and interlayer pores to the hydrates including the pores.

$$\phi_{ch} = \frac{\phi_{il} + \phi_{ig} + \phi_{ih}}{V_s} \tag{1}$$

where ϕ_{ch} is the intrinsic porosity, ϕ_{il} is the interlayer porosity [m^3/m^3], ϕ_{ig} is the intra-gel porosity [m^3/m^3], ϕ_{ih} is the inter-hydrate porosity [m^3/m^3], and V_s is the volume of hydrates including the interlayer, intra-gel, and inter-hydrate pores [m^3/m^3]. In the conventional DuCOM model [1], the intrinsic porosity is 0.28 [15] and, for the sake of simplicity, is a constant

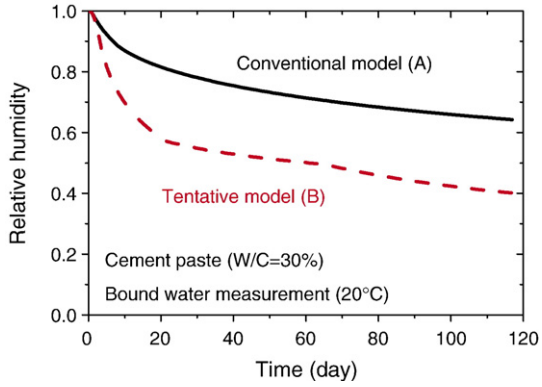

Fig. 4. Relative humidity under normal temperature condition (20 °C).

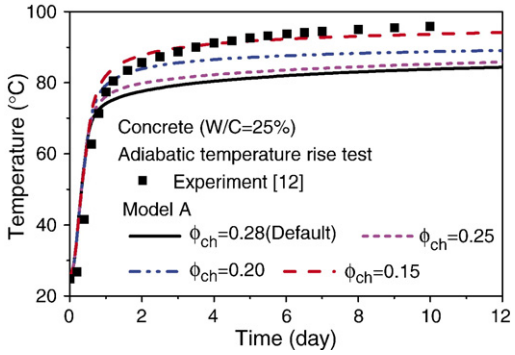

Fig. 5. Sensitivity analysis (intrinsic porosity).

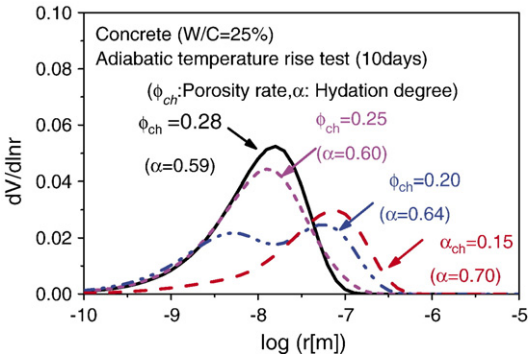

Fig. 6. Influence of intrinsic porosity on pore size distribution.

value independent of temperature. This value is equivalent to the minimum porosity that hydrate products cannot fill [9,15].

2.3. Sensitivity analysis as preparation for modification

Table 3 summarizes the current issues regarding the calculations for low W/C. Neither Model A nor Model B can explain the overall behavior of low W/C concrete under different experiment conditions. A method that has wide applicability for evaluating the overall behavior of concrete under various environmental conditions needs to be established.

In this section, the parameters that need to be improved in terms of their temperature dependencies on the hydration process are investigated by means of sensitivity analysis. In other words, the effect of the parameters on cement hydration, microstructure formation, and moisture profile are numerically discussed. In the analytical scheme, the strong interrelationships among the cement hydration, the micro-pore structure development, and the moisture transport/equilibrium are taken into account by real-time sharing of the material characteristic variables across each model. Therefore, the influence of a certain parameter in each model on the overall behavior is automatically considered.

Through the sensitivity analysis, it is found that the following parameters have strong influence on the concrete performance under different temperature conditions.

2.3.1. Intrinsic porosity

Many researchers have reported that a coarser microstructure is formed under higher curing temperatures when W/C is relatively high [4–6]. The reason is thought to be due to the formation of a dense hydrate layer around the cement particle under high temperatures. This temperature effect on the microstructure can be expressed by the decrease in the intrinsic porosity in the numerical analysis. In other words, a decrease in the intrinsic porosity under high temperatures is assumed in the sensitivity analysis. When the intrinsic porosity decreases, denser hydrate product is formed near the cement particles, and coarser capillary pores remain distant from the cement particles.

In the sensitivity analysis, constant porosities are assumed as a first approximation throughout the hydration process. Fig. 5 shows the results of an analysis of T25 using Model A. The smaller intrinsic porosity produced the higher temperature rise in the final stage.

Fig. 6 shows the computed pore size distribution after 10 days. When the intrinsic porosity was assumed to decrease under high curing temperatures, the microstructure did not become dense despite the increase in the degree of hydration. The decrease in the intrinsic porosity causes the decrease in intra-gel and inter-hydrate porosity and the increase in capillary porosity. Since the change in the microstructure affects the moisture distribution, the amount of free water in the capillary pore increases as the intrinsic porosity decreases. As a result, the shortage of free water was resolved and the large temperature rise was simulated.

In addition, when the intrinsic porosity decreased, the relative humidity did not decrease very much despite the large increase in the degree of hydration (Fig. 7). This was caused by the increase in the size of the pores at the liquid–vapor interface due to the decrease in intra-gel and inter-hydrate porosity. These results were calculated by taking into consideration the strong interrelationship of microstructure formation, moisture distribution, and cement hydration.

2.3.2. Inkbottle effect

Based on the results of experiments, the enhanced moisture model has been proposed as a way to simulate the temperature dependency of the stability of water trapped by the inkbottle effect associated with the microstructure [3]. Since the temperature rose to around 95 °C in the adiabatic temperature rise test for T25, the temperature dependency of the moisture might be significant in the experiment. The sensitivity analyses were performed using Models A and B with two moisture models. The first is the conventional model that neglects the

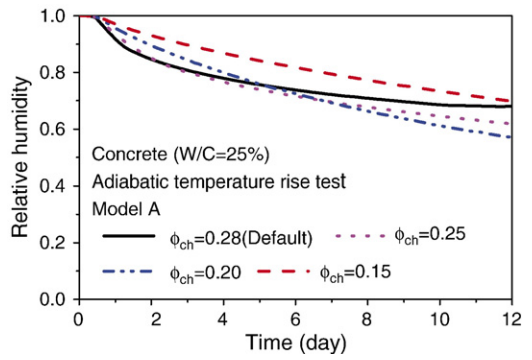

Fig. 7. Influence of intrinsic porosity on relative humidity.

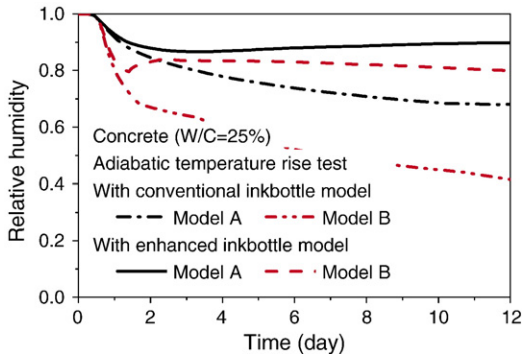

Fig. 8. Influence of inkbottle effect on relative humidity.

loss of trapped inkbottle water. The second is an enhanced model [3]. The analytical results for the hydration indicate that the different moisture models had no significant effect on the hydration process, since the amount of free water was almost the same. On the other hand, Fig. 8 shows that different moisture models had a strong effect on the relative humidity under high curing temperatures. The enhanced moisture model calculated the transfer of trapped inkbottle water from large pores to small pores under sealed conditions and high temperatures. As a result, the size of the pores at the liquid–vapor interface increased and the relative humidity also increased.

2.3.3. Interlayer water

It has been reported that the dispersion of interlayer water is significant under high temperatures [3]. An enhanced model for this phenomenon is also proposed based upon the experimental results [3]. Sensitivity analyses were performed to compare the conventional model and the enhanced model in both Models A and B. The results of these analyses are shown in Fig. 9. The reason for the difference was the increase in the amount of free water. This increase was caused by a decrease in the amount of interlayer water, which cannot be used for hydration, as well as the increase in the amount of water in the intra-gel, inter-hydrate and capillary pores. Since the tentative Model B treated a part of the water in the inter-hydrate pores as free water for hydration, it calculated a large amount of generated heat. In addition, the increased amount of water in the intra-gel, inter-hydrate and capillary pores greatly reduced the relative humidity (Fig. 10).

2.3.4. Minimum radius of pores for hydration

The minimum radius of the available space in an inter-hydrate pore for hydrate precipitation (*hydRmin*) is an important parameter to calculate the amount of free water for hydration (see Section 2.2.1). It was assumed to be 1.0 nm in Model B, which was proposed based on a sensitivity analysis by Kishi et al. [7]. The sensitivity analysis indicated that an inter-hydrate pore behaves as part of the available space for hydrate precipitation in the case of low W/C concrete [7], although the inter-hydrate pore was originally determined to be one of the gel pores in the conventional DuCOM model [1] where hydrate cannot precipitate. This idea is based upon research done by Powers and Brownyard [8,15]. While the specimens in the discussion by Kishi et al. were tested under adiabatic

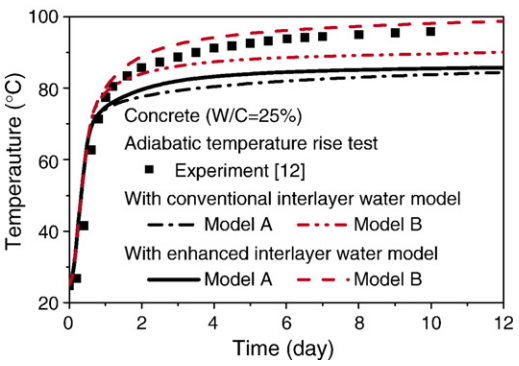

Fig. 9. Sensitivity analysis (enhanced interlayer water model).

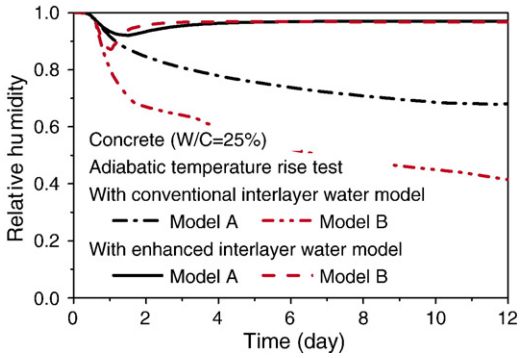

Fig. 10. Influence of interlayer water on relative humidity.

temperature conditions [7], the specimens in Powers' study were cured under normal temperature conditions [15]. Therefore, the reason for the different hydration functions of the inter-hydrate pores in the two studies is thought to be temperature dependency; the increase in temperature causes a decrease in the minimum radius of the available space for hydration. In this paper, the sensitivity analysis for the minimum radius is calculated for Y30 using Model B.

The results of the sensitivity analysis in this study show that an increase in the minimum radius reduced cement hydration (Fig. 11). When the minimum radius is 50 nm, the calculated result agrees with experiment's result. In this calculation, hydrate almost fails to precipitate in the inter-hydrate pores. The decrease in the relative humidity is also reduced by the increase in the minimum radius of the available space, as shown in Fig. 12. This is caused by the reduced hydration.

2.4. Summary of the sensitivity analysis

The results of the sensitivity analysis in this section can be summarized as following.

- In the conventional Model A, where the applicability to normal temperature conditions has been verified, the adiabatic temperature rise can be accurately simulated by the modification considering the decrease in the intrinsic porosity of hydrate under high curing temperatures (Result A).
- In the tentative Model B, where the applicability to adiabatic temperature conditions has been verified, the amount of

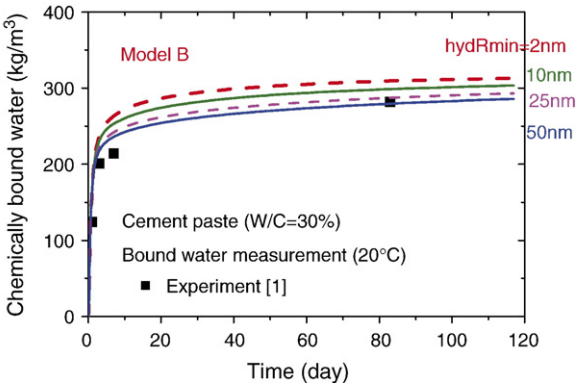

Fig. 11. Sensitivity analysis (minimum radius of available space for hydration).

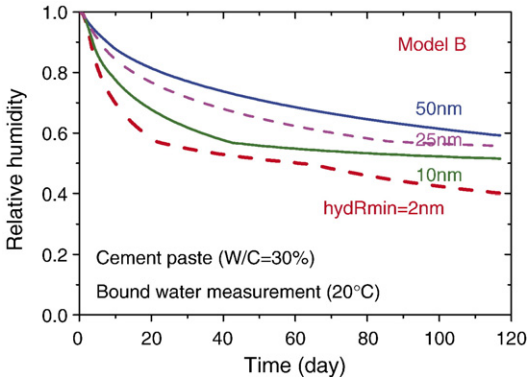

Fig. 12. Influence of minimum radius of available space on relative humidity.

chemically bound water under normal temperature conditions can be accurately calculated by the modification considering the increase in the minimum pore radius of the available space in inter-hydrate pores for hydrate precipitation (Result B).

- The computed relative humidity in adiabatic temperature conditions is high in the enhanced moisture model whereas the conventional model underestimated the relative humidity.

3. Enhanced modeling in terms of temperature dependency

Applying the results of the sensitivity analysis in the preceding section, this section proposes an enhanced model for temperature dependency on the microstructure. The proposed model consists of two temperature-dependent models; the intrinsic porosity of the hydrate and the minimum pore radius of the available space for hydrate precipitation in inter-hydrate pores. In the proposed model, the increase in the curing temperature causes a decrease in the intrinsic porosity based on the result A of the sensitivity analysis, and the number of capillary pores remaining increases. Since the amount of free water in the capillary pores increases under sealed conditions, cement hydration of low W/C continues for a longer period. Once the capillary pores are filled with cement hydrates, the precipitation of new hydrates may start in the inter-hydrate pores under high temperatures based on the result B of the sensitivity analysis. As a result, continuous hydration under high temperature is computed. The modified moisture models for inkbottle water and interlayer water are used in the computation.

3.1. Temperature-dependent model for the intrinsic porosity of the hydrate

The temperature-dependent model for the intrinsic porosity of the hydrate is formulated. When the curing temperature is 30 °C or lower (normal temperature), the intrinsic porosity in the proposed model is assumed to be 0.28, which is consistent with the value in the conventional model based upon research by Powers [15]. When the curing temperature increases, the porosity decreases. Here, the decrease in the inter-hydrate porosity is implicitly assumed to be the decrease in the porosity under high temperatures. When the curing temperature is 60 °C or higher, the porosity is assumed to be 0.20. The inflection points are at 30 and 60 °C since the results of the experiment [16], which will be discussed later in this paper, indicate a strong temperature dependency between 40 and 60 °C. The minimum value of porosity at high temperature is determined to be 0.20 by considering the results of sensitivity analysis. Here, the varying intrinsic porosity associated with the cement hydration in progress was investigated on the adiabatic temperature rise and relative humidity.

3.2. Temperature-dependent model for the minimum radius of free space for hydration

The temperature-dependent model is proposed for the minimum pore radius of the available space for hydrate precipitation in inter-hydrate pores. When the curing temperature increases, the minimum radius decreases. When the curing temperature is 30 °C or lower, the minimum radius is assumed to be 50 nm. This means that the hydrate product almost fails to precipitate in the inter-hydrate pores at normal curing temperatures. When the curing temperature is 60 °C or higher, the minimum radius is assumed to be 2 nm, which is the boundary between intra-gel and inter-hydrate pores described in Section 2.1. The inflection points are the same as ones in the temperature-dependent model for the intrinsic porosity.

3.3. Calculating the microstructure

Based on the average hydration degree of powder and the amount of bound water calculated by the hydration model, the pore size distribution over time is calculated using the microstructure model. This section explains the two stages of the procedure in the proposed computations (Fig. 13).

3.3.1. Calculating the porosity of the first stage (hydrate precipitation into capillary pores)

First, the total volume of the hydrate products, including the interlayer and the intra-gel and inter-hydrate pores, is

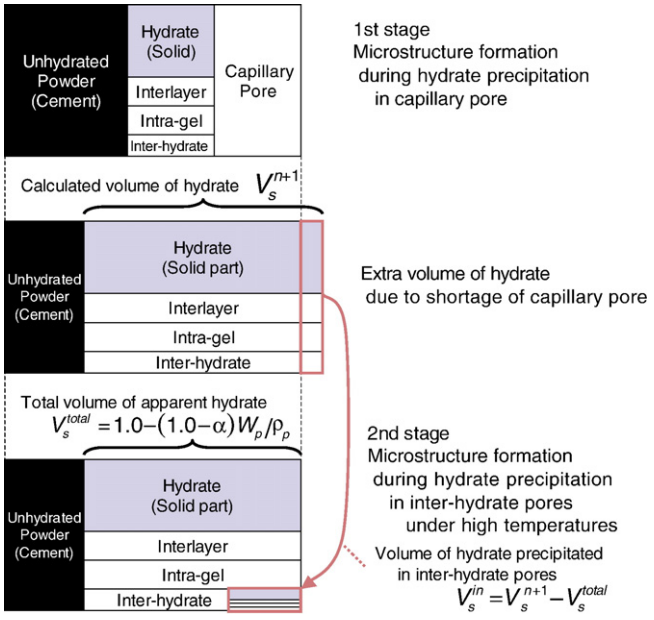

Fig. 13. Computations of microstructure formation in proposed model.

calculated. Since the intrinsic porosity varies with temperature in the proposed model, the calculation must consider the temperature history with hydration process over time. The total volume in a unit of cement paste is calculated by accumulating the incremental changes in volume over time.

$$V_s^{n+1} = V_s^n + \Delta V_s \tag{2}$$

where V_s^{n+1} and V_s^n are the total volume [m^3/m^3] of hydrate in the $n+1$th and nth step respectively, and ΔV_s is the increased volume [m^3/m^3] from the nth step to the $n+1$th step. The increased volume at any arbitrary stage of hydration can be obtained as follows.

$$\Delta V_s = \frac{1}{1-\phi_{ch}^{n+1}}\left(\frac{\Delta\alpha \cdot M_p}{\rho_p} + \frac{\Delta M_{chem}}{\rho_u}\right) \tag{3}$$

where ϕ_{ch}^{n+1} is the intrinsic porosity for the temperature at the $n+1$th step, $\Delta\alpha$ is the increased average degree of hydration from the nth step to the $n+1$th step, M_p is the mass of the powder materials per unit of paste volume, ρ_p is the density of the powder materials, ΔM_{chem} is the increased mass of the chemically bound water from the nth step to the $n+1$th step and ρ_u is the density of the chemically bound water ($=1.25\times10^3$ kg/m^3). The changes of hydration degree and bound water are calculated by the hydration model based on reaction kinetics over time. The capillary porosity at $n+1$th step, ϕ_c^{n+1}, can be calculated from the overall volume balance of the paste as follows

$$\phi_c^{n+1} = 1 - V_s^{n+1} - (1-\alpha)\frac{M_p}{\rho_p} \tag{4}$$

3.3.2. Calculating the porosity of the second stage (hydrate precipitation into inter-hydrate pores)

When the value of the capillary porosity is negative in the above computation, the following additional calculation is necessary to compute the precipitation of the hydrate products into the inter-hydrate pores as shown in Fig. 13. This computation of the second stage is based upon the temperature-dependent model for the minimum radius of the available space only when the concrete containing the inter-hydrate pores for the precipitation is being cured at a high temperature.

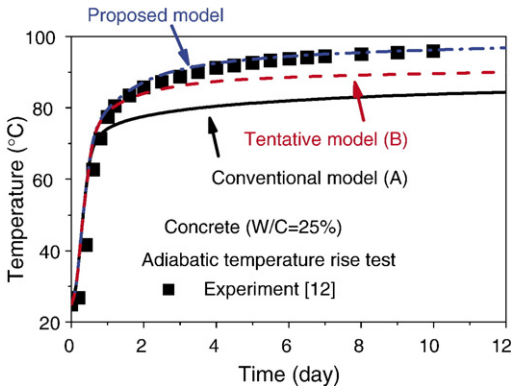

Fig. 14. Adiabatic temperature rise calculated by proposed model.

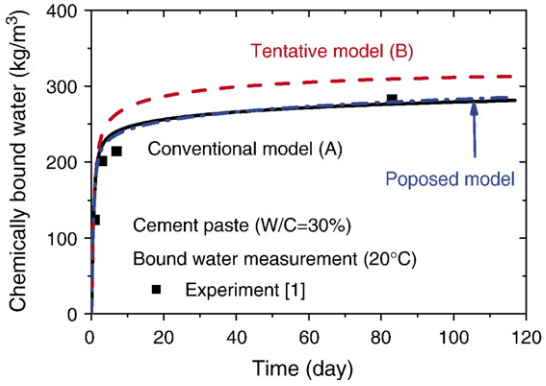

Fig. 15. Chemically bound water calculated by proposed model under normal temperature condition.

The extra hydrate that cannot precipitate in the capillary pores fills the free space in the inter-hydrate pores under high temperatures. This is based on the enhanced model that takes into account the minimum radius of the available space. As a result, the total volume of apparent hydrate products, including the interlayer and the intra-gel and inter-hydrate pores (V_s^{total}) becomes smaller than the total volume that is calculated by integrating the volume of the hydrate products (V_s^{n+1}). The apparent total volume V_s^{total} is equal to the volume of the paste excluding unhydrated powder materials.

$$V_s^{total} = 1 - (1-\alpha)\frac{M_p}{\rho_p} \tag{5}$$

The difference between V_s^{total} and V_s^{n+1} is the volume of hydrate that precipitates in the inter-hydrate pores. The extra volume V_s^{in} is calculated as follows.

$$V_s^{in} = V_s^{n+1} - V_s^{total} \tag{6}$$

3.3.3. Calculating pore size distribution

The surface area and the pore size distribution in the microstructure can be obtained from the porosities calculated above. The temperature dependencies of the average size and specific surface area of the hydrate products for calculating the surface area of pore are determined related to the minimum size of free space for hydration. Finally, the pore size distributions of the capillary, intra-gel, and inter-hydrate pores are represented by simplistic Rayleigh–Ritz (R–R) distribution functions [1]. Here, the intra-gel and inter-hydrate pores are treated by a shared distribution function for the sake of simplicity, as mentioned in the Section 2.1.

4. Numerical simulation

4.1. Hydration process under adiabatic and normal temperature conditions

The proposed model was verified with two types of experiments: the adiabatic temperature rise test (T25) and

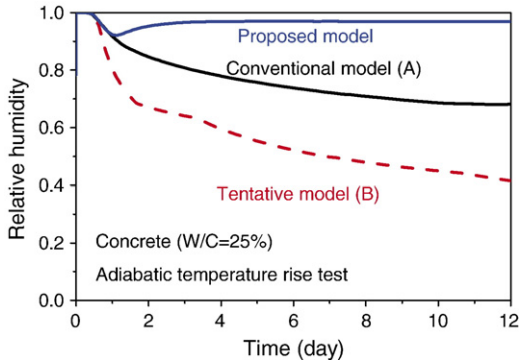

Fig. 16. Calculated relative humidity under adiabatic temperature condition.

measurement of the chemically bound water (Y30). Those experiments represent hydration processes under both high temperature and normal temperature conditions. Figs. 14 and 15 show the results of the experiments and analyses of the hydration process. Compared to the conventional model, the proposed model can accurately predict the results of both experiments under different temperature conditions. In the adiabatic temperature rise test, continuous hydration is simulated by the proposed model mainly for two reasons. The first is decrease in intrinsic porosity, which results in a larger amount of free water for hydration. The second is the increase in the space that is available for hydration under high temperatures. The decrease in the average intrinsic porosity in the adiabatic temperature test resulted in the formation of denser hydrate product near the cement particles. This result is consistent with the results of experiments using backscattered electron imaging that show lighter products forming under high curing temperatures [6].

For the bound water measurements, both the proposed and conventional models give reasonable analytical results, since the conventional model has been verified by experiments at normal temperatures (mainly 20 °C).

Figs. 16 and 17 show the results of an analysis of the changes in relative humidity inside the specimen. In adiabatic temperature conditions, the decrease in the relative humidity calculated by the proposed model was very small. The calculated relative humidity at 12 days was around 95%. Although there is no data from experiments that directly verify these results, the following two experiments indirectly validate the calculation. The first experiment investigated the effect of the curing temperature on the relative humidity [14]. In this study, the relative humidity was measured at temperatures of 20, 40, and 60 °C. The results show that the relative humidity increases as the curing temperature rises. The relative humidity at 2 days was around 90% at 60 °C. Since the maximum temperature in the adiabatic temperature test was around 95 °C, the small decrease in the calculated relative humidity under adiabatic conditions seems to be validated. The second experiment was a trial in this study. The authors measured the relative humidity under quasi-adiabatic temperature conditions. The relative humidity at the center of specimen was measured at the center point of a cube specimen whose sides were 400 mm. The specimen was covered with Styrofoam having a thickness of 100 mm. The measured relative humidity was 100% during the 7-day experiment, although the value is too high to ensure the accuracy of the measuring device.

In the sealed condition at 20 °C, the results of the analysis showed a decrease in the relative humidity similar to that seen in the experiment, although the decrease in the analysis was a little bit greater than it was in the experimental result. In this paper, the experiment measured the mortar in W/C 30% cement [17], which is equal to the water-to-cement ratio calculated in this study.

4.2. Hydration process under late-elevated temperature conditions

This section investigates the effect of late-elevated temperatures on the hydration process of the cementitious materials, which were sufficiently cured under normal temperatures in advance. Two different curing temperature histories were adopted in the experiment. In the first experiment (P25a), a constant temperature of 20 °C was given. In the second experiment (P25b), ambient temperature was elevated instantaneously from 20 °C to 60 °C at the age of 15 days, and then temperature was further elevated from 60 °C to 80 °C at the age of 33 days. The bound water was measured in cylindrical specimens having a radius of 100 mm and a height of 200 mm. The mix proportion is shown in Table 2. The specimens were cured under sealed conditions until they were measured. They were then broken, and samples of about 20 mg were collected

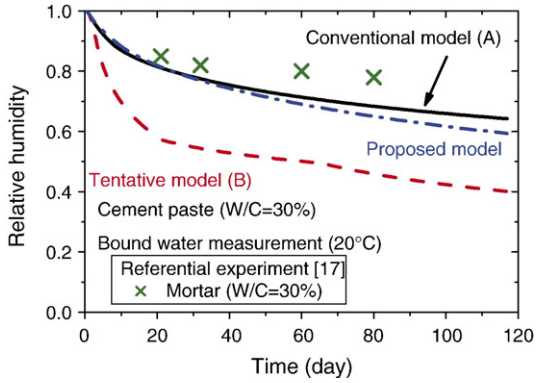

Fig. 17. Calculated relative humidity under normal temperature condition.

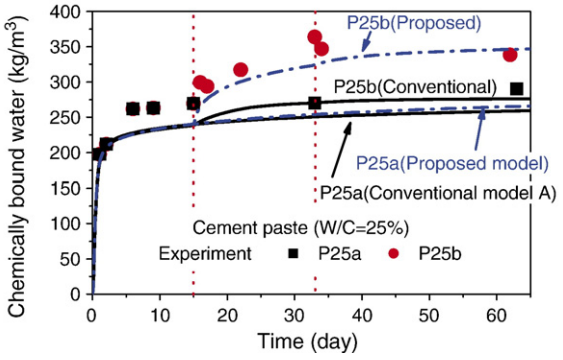

Fig. 18. Change of bound water under late-elevated temperature condition.

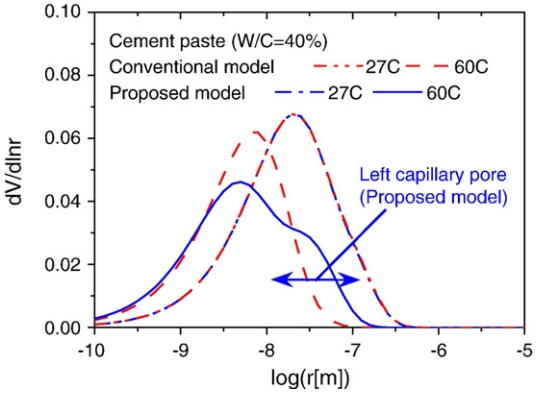

Fig. 19. Pore size distribution in case of normal W/C (calculation).

for thermo gravimetric analysis (TGA). In the TGA, the temperature was increased in steps of 10 °C up to 100 °C, where it was kept constant for 5 min. Subsequently, the temperature was increased at a rate of 10 °C/s up to 1200 °C. The loss of mass in the sample between 100 °C and 1000 °C was considered to be caused by the loss of unevaporable bound water. Fig. 18 shows the results of the experiment and analysis. The experiment revealed a large increase in the amount of bound water due to the increase in the curing temperature. While the conventional model underestimated the large increase in the bound water under the elevated temperature conditions, the proposed model could accurately predict the hydration process in the experiment. In the proposed calculation, the increase in the available space for hydration under high temperatures resulted in additional hydration. In this case, the decrease in the intrinsic porosity under elevated temperatures did not contribute to an increase in hydration since almost no capillary pores remained.

4.3. Influence of curing temperature on the microstructure (normal W/C)

This section describes the influence of high-temperature curing on the formation of the microstructure in cement paste having a normal W/C. In this paper, normal W/C means a W/C with enough free water for hydration (around 40% or more). It is well known that the microstructure becomes coarser due to the high curing temperature. Goto and Roy reported the results of an experiment in which the pore size distribution was measured using the MIP method [5]. The specimens (W/C=40%) were cured at either a normal temperature (27 °C) or a high temperature (60 °C) for 4 weeks. In the case of high temperature curing, the fine porosity on a 10^{-9} m-scale was higher and the coarse porosity on a 10^{-7} m-scale lower than was seen in the case of normal temperature curing. Fig. 19 shows the analytical results. In the conventional model, the microstructure became dense under high temperature curing since degree of hydration was high. No large capillary pores remained. On the other hand, in the proposed model, a coarse microstructure was observed in

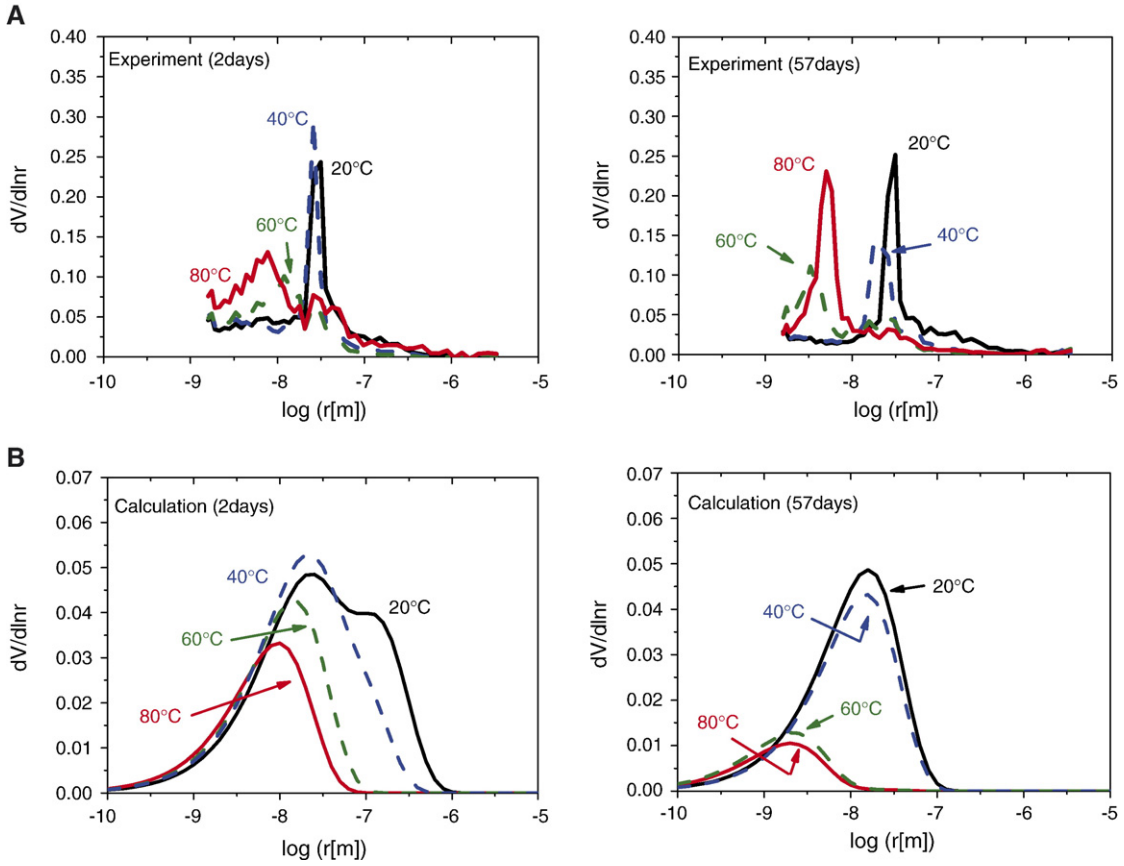

Fig. 20. A. Pore size distribution of low W/C cement paste (experiment [16]). B. Pore size distribution of low W/C cement paste (calculation).

the case of high temperature curing. The decrease in the intrinsic porosity under high temperatures produces an increase in the number of large capillary pores. The increase in available space for hydration under high temperature curing did not affect the hydration process since an adequate volume of capillary pores remained.

4.4. Influence of curing temperature on the microstructure (low W/C)

This section describes the influence of high temperature curing on the formation of the microstructure in cement paste having a low W/C. Ito et al. measured the pore size distribution of cement paste (W/C=25%) under different temperature histories [16]. After first curing at 20 °C for 24 h, four temperature conditions (20, 40, 60 and 80 °C) were applied as environmental conditions. The specimens were sealed to prevent moisture loss. At 2 and 57 days after the casting of specimens, the specimens were broken, and the pore size distributions were measured using the MIP method. The mix proportion is shown in Table 2.

Fig. 20A shows the results of experiments conducted by Ito et al. [16]. At 20 and 40 °C, the peaks of the pore size distributions were observed between 10^{-8} m and 10^{-7} m, and the porosity decreased as hydration proceeded. On the other hand, At 60 and 80 °C, the peaks of the pore size distributions were between 10^{-9} m and 10^{-8} m, which are smaller than they were at 20 and 40 °C.

Fig. 20B shows the results calculated by the proposed model. The proposed model can roughly simulate the different tendencies between normal temperature curing (20 and 40 °C) and high temperature curing (60 and 80 °C). However, the analysis does not precisely express the clear peak seen in the experiment. The reason for the gentle peak in the analysis is that the system used in the analysis represents the average pore size distribution by applying a simplistic Rayleigh–Ritz distribution function. Several verifications indicate that this simplification can still be applied to solving practical issues such as thermal stress, shrinkage, and mass transfer [1,2].

5. Conclusions

In this study, the basic models of the thermodynamic system were enhanced in order to extend their applicability to solving the practical issues of concrete under arbitrary ambient temperature conditions. Sensitivity analysis was used to investigate the influence of the temperature dependency of the material parameters on hydration degree, pore size distribution, and relative humidity. The proposed enhanced model introduces the temperature-dependent intrinsic porosity of the hydrates. In addition, the available space for hydrate precipitation is assumed to vary with the temperature. These enhancements, which are based upon the redefinitions of pores in the cement paste, were verified by experiments on adiabatic temperature rise, chemically bound water, relative humidity, and pore size distribution. As a result, the wide applicability of the proposed model was validated for arbitrary water-to-cement ratios under various temperature histories. In particular, the overall calculations for low W/C and high temperature curing were more accurate under the proposed model than under the conventional model. The concluding remarks are summarized below.

5.1. Normal temperature

The material performances of the concrete cured under normal temperature condition have been accurately simulated by the conventional model. The proposed model produces simulations that are equally accurate.

5.2. Late-elevated temperature

The hydration process under late-elevated temperatures was investigated. In case of normal W/C, the late-elevated temperature did not affect the hydration process since enough free water remains for hydration at normal temperatures. As a result, the hydration process in late-elevated temperature condition can be simulated in the same manner as in the normal temperature condition mentioned above. On the other hand, in case of low W/C, additional hydration was observed in late-elevated temperature curing. The proposed model can simulate the additional hydration process by considering the temperature dependency of the available space for hydrate precipitation. Specifically, the hydrate can precipitate in the inter-hydrate pores between the hydrate products under high temperatures.

5.3. High temperature in case of normal W/C

Although the applicability of the conventional model of the hydration process has been verified, the coarser microstructure cannot be simulated. In the proposed model, the coarser microstructure is expressed by the temperature dependency of the intrinsic porosity. The intrinsic porosity decreases at high temperatures. On the other hand, the change in the microstructure does not affect the hydration process since enough free water remains for hydration. Therefore, the conventional model of hydration remains in the proposed model.

5.4. High temperature in case of low W/C

The hydration of low W/C concrete under high temperatures differs from that of normal W/C. The proposed model can accurately predict the continuous hydration process by considering the temperature-dependent intrinsic porosity of the hydrate and the available space for hydrate precipitation. The proposed model also simulates the finer microstructure that forms during high temperature curing.

In the present computations of the porosity distributions, the intra-gel and inter-hydrate pores are treated together for the sake of simplicity. Through several verifications, it is thought that this simplified approach provides adequate accuracy and applicability for solving practical issues from an engineering viewpoint. On the other hand, it has been reported that the behaviors of the moisture in micro-pores strongly interact with the macroscopic behaviors of concrete materials [18]. In addition, in the case of concrete containing fly ash or blast-furnace slag that consumes CH, the

influence of the difference between the intra-gel and inter-hydrate pores is thought to be more significant [19] since the pore structure of the crystal containing no intra-gel pores differs from the other hydrates, including C–S–H gel [10]. Therefore, computational treatments of the porosity distributions in the intra-gel and inter-hydrate gel pores may require discussion in certain future research efforts.

References

[1] K. Maekawa, R.P. Chaube, T. Kishi, Modelling of Concrete Performance, E and FN SPON, London, 1999.

[2] K. Maekawa, T. Ishida, T. Kishi, Multi-scale modeling of concrete performance — integrated material and structural mechanics, J. Adv. Concr. Technol. 1 (2) (2003) 91–126.

[3] T. Ishida, K. Maekawa, T. Kishi, Enhanced modeling of moisture equilibrium and transport in cementitious materials under arbitrary temperature and relative humidity history, Cem Concr Res, submitted for publication to Monte Verita Conference special issue (submitted for publication).

[4] K.O. Kjellsen, R.J. Detwiler, O.E. Gjørv, Pore structure of plain cement pastes hydrated at different temperature, Cem. Concr. Res. 20 (6) (1990) 927–933.

[5] S. Goto, D.M. Roy, The effect of W/C ratio and curing temperature on the permeability of hardened cement paste, Cem. Concr. Res. 11 (1981) 575–579.

[6] C. Famy, K.L. Scrivener, A. Atkinson, A.R. Brough, Effect of an early or a late heat treatment on the microstructure and composition of inner C–S–H products of Portland cement mortars, Cem. Concr. Res. 32 (2002) 269–278.

[7] T. Kishi, T. Ishida, K. Maekawa, Interaction of hydration heat of low water to cement ratio concrete with moisture equilibrium in solid micro-pore, J. of Materials, Concrete Structure, Pavements, vol. 690/V-53, 2001, pp. 45–54.

[8] T.C. Powers, T.L. Brownyard, Studies of the physical properties of hardened Portland cement paste, Part 9, general summary of findings on the properties of hardened Portland cement paste, J. Am. Concr. Inst. 18 (8) (1947) 972–992.

[9] H.F.W. Taylor, Cement Chemistry, Second edition, Thomas Telford, London, 1997, pp. 231–237.

[10] M. Daimon, S.A. Abo-El-Enein, G. Hosaka, S. Goto, R. Kondo, Pore structure of calcium silicate hydrate in hydrated tricalcium silicate, J. Am. Ceram. Soc. 60 (3–4) (1977) 110–114.

[11] H. Uchikawa, S. Uchida, S. Hanehara, Measuring method of pore structure in hardened cement paste, mortar and concrete, vol. 88, il Cemento, 1991, pp. 67–90.

[12] K. Taniguchi, T. Kishi, T. Ishida, Moisture behavior during cement hydration, Proc. Jpn. Soc. Civ. Eng. 55 (5) (2000) 510–511.

[13] B. Persson, Moisture in concrete subjected to different kinds of curing, Mat. Struct. 30 (1997) 533–544.

[14] K.B. Park, T. Noguchi, Autogenous shrinkage of cement paste hydrated at different temperatures: influence of microstructure and relative humidity change, in: B. Persson, G. Fagerlund (Eds.), Proc. of the 3rd Int'l Res. Sem. on Self-Desiccation and its Importance in Concrete Technology, Lund, Sweden, 2002, pp. 93–101.

[15] T.C. Powers, The physical structure of Portland cement paste, in: H.F. Taylor (Ed.), The Chemistry of Cement, Academic Press, New York, 1964, pp. 391–416.

[16] K. Ito, T. Kishi, T. Uomoto, Microstructure of hardened cement paste formed in various curing temperature, Proc. Jpn. Concr. Inst. 24 (1) (2002) 489–490.

[17] A.M. Paillere, M. Buil, J.J. Serrane, Effect of fiber addition on the autogenous shrinkage of silica fume concrete, Discussion, Author's Closure, ACI Material, vol. 87(1), 1990, pp. 82–83.

[18] S. Asamoto, T. Ishida, K. Maekawa, Time-dependent constitutive model of solidifying concrete based on thermodynamic state of moisture in fine pores, J. Adv. Concr. Technol. 4 (2) (2006) 301–323.

[19] K. Nakarai, T. Ishida, T. Kishi, K. Maekawa, Enhanced modeling of microstructure formation of cement hydrates coupled with thermodynamics, Proc. of Workshop on Cementitious Materials as Model Porous Media: Nanostructure and Transport Processes, 2005, pp. 147–151.